Generalized radiation law for excited media in a nonequilibrium steady state

F. Richter,* M. Florian, and K. Henneberger
Institut für Physik, Universität Rostock, 18051 Rostock, Germany

(Received 26 January 2007; revised manuscript received 15 October 2008; published 20 November 2008)

We consider the interacting system of light and matter and present quantum-kinetically exact relations for the propagation of light through arbitrarily absorbing and dispersive steadily excited media in a specified geometry. We arrive at an energy flow law which may be regarded as a generalization of the Kirchhoff and Planck radiation laws to nonequilibrium. The field fluctuations are shown to generally split up into medium- and vacuum-induced contributions, of which only the latter governs the energy transport between the medium and the environment. A thorough derivation of the law is given and it is discussed together with interesting details in the underlying relations and physics. Especially, in the context of excited semiconductors, quasiequilibrium emission and lasing, as well as spectral features in the presence of quantum condensation are addressed.

DOI: 10.1103/PhysRevB.78.205114 PACS number(s): 42.50.Ct, 42.50.Nn, 78.45.+h, 78.20.−e

I. INTRODUCTION

Light propagating through matter is subjected to manifold interactions through the coupling of the electromagnetic fields to charged particles, rendering its description as a highly complex problem. Matter coupled to light has to be considered as a dynamic many-body system and the entire problem is to be treated quantum mechanically.

One successful technique that allows for a quantum-kinetically consistent treatment of a many-body system interacting with electromagnetic fields is the Green's function (GF) technique and its nonequilibrium generalization.[1–3] In Refs. 4 and 5, the microscopic theory of semiconductor lasers was extended to nonequilibrium quantum mechanics using the Keldysh technique. A set of exact relations could be derived and the emission of excited semiconductors and semiconductor lasers was analyzed. These results were given in terms of bulk-matter functions (dielectric function and generation rate), neglecting any effects of spatial dispersion (SD) or spatial inhomogeneities.

Since these appear in principle in any nonbulk matter, e.g., a semiconductor slab, further efforts on this topic have been made. Eventually, spatial inhomogeneities could be fully accounted for in slab geometry, and an exact theory for the propagation of light through arbitrarily absorbing and dispersive media in a nonequilibrium steady state was developed. A brief overview of the general theory was presented in Ref. 6.

This theory also yields a general law for the energy flow between media in a nonequilibrium steady state, to which led some inspiring ideas from Ref. 7. Its validity extends far over semiconductor lasers due to the universality of the Green's function approach. The properties of the medium enter the theory only via the dielectric function, which can be modeled for the system considered. The law can be regarded as a generalization of the Kirchhoff and Planck radiation laws to arbitrary nonequilibrium states.

This paper aims to give a thorough derivation of this theory preceded by a general overview of the energy flow law, which is readable for nonspecialists too, and an extensive discussion of the theory in the context of excited semiconductors, lasing, and quantum condensation. Several example cases have been calculated and illustrative plots are shown.

The theory part is laid out as follows. First we try to illustrate the Green's function concept and its main ingredients so that the following theoretical treatise can be followed easier. In Sec. III B we tailor the *photon Green's function* (PGF) to the slab geometry. After the solution structure for the vector potential is introduced, we start considering the energy conservation on the basis of Poynting's theorem (Sec. III E), which we formulate at first for classical light, then in terms of the photon Green's functions and the vector potential. This results in the energy flow law, whose physical contents are then discussed in Sec. IV.

II. OVERVIEW OF THE THEORY

If a body itself is in thermal equilibrium and also in thermal equilibrium with the surrounding vacuum, the radiation emitted by the body s_e is equal to the absorbed radiation s_a and there is no resulting energy flow,

$$s(\omega,\alpha) = s_e(\omega,\alpha) - s_a(\omega,\alpha) = 0. \tag{1}$$

For this case, the Kirchhoff law states that the emission is proportional to the absorptivity a of the body, i.e., the fraction of light intensity which the body absorbs if irradiated with light. For a *blackbody*, $a \equiv 1$; but in general, a will depend on the frequency ω of the radiation and the angle of observation α. The state of the body may play a role too, and a dependence of a on material parameters such as the temperature can be assumed but is not written out in the following.

Kirchhoff also knew that the proportionality factor n, later called the "Kirchhoff function," must be a universal function of ω and the temperature T of the system,[8]

$$s_e(\omega,\alpha) = s_a(\omega,\alpha) = n(\omega,T)a(\omega,\alpha). \tag{2}$$

The absorptivity is easily accessible to measurements, e.g., for a medium with plane-parallel surfaces using the energy conservation equation

$$a(\omega,\alpha) = 1 - |r(\omega,\alpha)|^2 - |t(\omega,\alpha)|^2, \tag{3}$$

where r,t are the reflectivity and transmittivity of the body for incident light normalized to unity. The concrete form of the Kirchhoff function was subjected to intense scientific debate until Planck presented his well-known formula for the spectral radiance in thermal equilibrium,[9] which corresponds to n being a Bose function

$$n(\omega,T) = \frac{1}{\exp\left[\frac{1}{k_B T}(\hbar\omega - \mu)\right] - 1} \tag{4}$$

with vanishing chemical potential $\mu=0$.

In this paper, we will show that these relations can be generalized as follows for "slab geometry," i.e., if a medium which is infinitely extended in the y-z direction is assumed. Both the medium and its environment may be in arbitrary nonequilibrium steady states. Then, the energy flow will not generally vanish: $s=s_e-s_a\neq 0$. The absorbed energy s_a is still given by the absorptivity a, but the function $n(\omega,\alpha)$ now is an arbitrary function reflecting the nonequilibrium distribution of photons in the environment ("photon bath"). In this generalized Kirchhoff function, an angle dependence has to be included, and there is no temperature dependence in the sense that the temperature is not defined in a nonequilibrium system.

While in Kirchhoff's original law the emission is only accessible via the absorption in thermal equilibrium, we can now establish an independent relationship for it. Curiously, even though the emission is a pure quantum effect, it can be shown to be given by the (purely classical) absorptivity a. The corresponding proportionality factor $b(\omega,\alpha)$ reflects the nonequilibrium distribution of medium-induced *optical* excitation, or "internal photons," which is coupled to the *medium* excitation. In a semiconductor, e.g., these excitations are polaritons and excitons, respectively.

Thus, the generalized energy flow law can be written in the compact form

$$s(\omega,\alpha) = [b(\omega,\alpha) - n(\omega,\alpha)]a(\omega,\alpha). \tag{5}$$

The full energy flux density (Poynting vector) in x direction is then given as the integral over these spectrally and angular resolved quantities,

$$S_x = \int d\alpha \int \frac{d\omega}{2\pi}\hbar\omega s(\omega,\alpha). \tag{6}$$

Furthermore, if the medium can be assumed to be in a quasiequilibrium state, b develops into a Bose function in which the chemical potential μ becomes a measure for the medium excitation. Medium-induced optical excitations are thus, in a sense, always bosonic even though they are coupled to fermionic matter.

III. THEORY

A. Photon Green's function technique

GFs, as known from mathematics, are used to solve inhomogeneous differential equations, e.g., in classical electrodynamics. In the quantum-mechanical Green's function theory, they are usually defined as an expectation value of field operator correlations in the Heisenberg picture. A certain kind of these GFs obeys a wave equation with a δ inhomogeneity and thus formally resembles the mathematical Green's function.

This concept proved quite successful for equilibrium systems and is widely used, e.g., in thermodynamics. In a nonequilibrium system however, time ordering of operators for forward or backward evolution becomes crucial. The Keldysh technique[3,10] takes this problem into account by defining Green's functions on a double-time contour $\mathcal{C}$, which allows keeping a close formal analogy to the equilibrium case.

Corresponding to the four possible time orders in an operator correlation, the contour-ordered Green's function contains four different physical functions with different physical contents.[11,12] These so-called Keldysh components are $G^{>},G^{<},G^{++},G^{--}$, of which only two are independent, so that several general identities exist between them (see Appendix A).

The "greater" and "less" functions are often called as "correlators" and are directly linked to particle densities, currents, and fluctuations. Additionally, one usually defines the "retarded" and "advanced" functions $G^{\mathrm{ret}},G^{\mathrm{adv}}$, which can be used to calculate responses to perturbations of the system, and the spectral function $\hat{G}$, which describes spectral properties. For example, the particle density can be expressed as a frequency integral over $\hat{G}$ times the Wigner function. The latter is the representation of the single-particle density matrix and closely related to $G^{<}$. In the equilibrium limit, this relation yields the well-known Fermi particle density.[2] For further details on the technique, we recommend Ref. 12; for application to nonideal plasmas in general, Ref. 13; and for application to the coupled system of radiation and matter, Refs. 11, 14, and 15. Introductions are given, e.g., in Refs. 5 and 16.

While the particle Green's function is usually denoted by G, the PGF in a many-particle system coupled to electromagnetic fields is the one defined in terms of the vector potential operator $\hat{\mathbf{A}}$ and is denoted by D. We will now sum up how some important relations for photon Green's functions evolve. The effective vector potential in Coulomb gauge on the double-time contour $\mathbf{A}_{\mathrm{eff}}(\underline{1})=\langle\hat{\mathbf{A}}(\underline{1})\rangle_{\mathcal{C}}$, where $\underline{1}$ is the parameter tuple $(\mathbf{r}_1,\underline{t}_1)$ and $\underline{t}$ denotes a time on the contour, obeys Maxwell's potential equation in its usual form

$$\left(\Delta - \frac{1}{c^2}\frac{\partial^2}{\partial \underline{t}^2}\right)\mathbf{A}_{\mathrm{eff}}(\mathbf{r},\underline{t}) = -\mu_0[\mathbf{j}_{\mathrm{ind}}(\mathbf{r},\underline{t}) + \mathbf{j}_{\mathrm{ext}}(\mathbf{r},\underline{t})], \tag{7}$$

where $\mathbf{j}_{\mathrm{ind}}=\langle\hat{\mathbf{j}}\rangle_{\mathcal{C}}$ and $\mathbf{j}_{\mathrm{ext}}$ is a c-number function.

First we define the photon GF $D(\underline{1},\underline{2})$ as the functional derivative

$$D_{ik}(\underline{1},\underline{2}) = -\frac{1}{\mu_0}\frac{\delta A_{\mathrm{eff},i}(\underline{1})}{\delta j_{\mathrm{ext},k}(\underline{2})} = -\frac{1}{\mu_0}\frac{\mathrm{i}}{\hbar}\{\langle\hat{A}_i(\underline{1})\hat{A}_k(\underline{2})\rangle_{\mathcal{C}} - A_{\mathrm{eff},i}(\underline{1})A_{\mathrm{eff},k}(\underline{2})\}, \tag{8}$$

which contains the above-mentioned operator correlations or

more specifically field-field fluctuations (i,k denote vector components).[14] Second, the *polarization function* P ("photon self-energy") is defined as

$$P_{ik}(\underline{1},\underline{2}) = -\mu_0 \frac{\delta j_{\mathrm{ind},i}(\underline{1})}{\delta A_{\mathrm{eff},k}(\underline{2})}, \tag{9}$$

so that the chain rule yields

$$\frac{\delta j_{\mathrm{ind},i}(\underline{1})}{\delta j_{\mathrm{ext},k}(\underline{2})} = P_{il}(\underline{1},\underline{3})D_{lk}(\underline{3},\underline{2}). \tag{10}$$

Here and in what follows, the *sum convention* is applied.

The photon self-energy couples the light to the matter subsystem. It is the only point where the medium properties enter. Because quantities that cannot be determined exactly are combined into this single quantity, approximations are automatically consistent. This avoids unbalanced approximations, which may give rise to artifacts that obscure or distort physical effects. However, the problem remains to find an approximation for the photon self-energy which reproduces the physics of interest well enough.

Carrying out the derivative $\delta/\delta j_{\mathrm{ext}}$ in the potential equation, we arrive at the *Dyson equation* for the photon GF

$$\{D^{0,-1}_{ij}(\underline{1},\underline{2}) - P_{ij}(\underline{1},\underline{2})\}D_{jk}(\underline{2},\underline{3}) = \delta(\underline{t}_1 - \underline{t}_3)t_{ik}(\mathbf{r}_1 - \mathbf{r}_3) \tag{11}$$

with the *inverse free* photon GF

$$D^{0,-1}_{ij}(\underline{1},\underline{2}) = \left(\Delta_{\mathbf{r}_1} - \frac{1}{c^2}\frac{\partial^2}{\partial \underline{t}_1^2}\right)\delta(\underline{1}-\underline{2}) \tag{12}$$

and the transverse δ function[5]

$$t_{ij}(\mathbf{r}-\mathbf{r}') = \delta_{ij}\delta(\mathbf{r}-\mathbf{r}') + \nabla_i\nabla_j\frac{1}{4\pi|\mathbf{r}-\mathbf{r}'|}. \tag{13}$$

Extracting the Keldysh components of this contour-ordered equation, one finds for the retarded and advanced GFs, which are defined as

$$D^{\mathrm{ret}}_{ij}(1,2) = \Theta(t_1 - t_2)\{D^{>}_{ij}(1,2) - D^{<}_{ij}(1,2)\}, \tag{14}$$

$$D^{\mathrm{adv}}_{ij}(1,2) = D^{\mathrm{ret}}_{ji}(2,1), \tag{15}$$

the retarded Dyson equation

$$D^{\mathrm{ret},-1}_{ik}(1,2)D^{\mathrm{ret}}_{ij}(2,3) = \delta(\underline{t}_1 - \underline{t}_3)t_{ij}(1-3), \tag{16}$$

$$D^{\mathrm{ret},-1}_{ik}(1,2) = D^{0,\mathrm{ret},-1}_{ik}(1,2) - P^{\mathrm{ret}}_{ik}(1,2), \tag{17}$$

$$D^{0,\mathrm{ret},-1}_{ik}(1,2) = \left(\Delta_{\mathbf{r}_1} - \frac{\partial^2}{\partial t_1^2}\right)\delta(1-2), \tag{18}$$

and for the correlators the so-called *kinetic* Dyson equation

$$D^{\mathrm{ret},-1}_{ik}(1,2)D^{\gtrless}_{kj}(2,3) - P^{\gtrless}_{ik}(1,2)D^{\mathrm{adv}}_{kj}(2,3) = 0. \tag{19}$$

Multiplication with D^{ret} yields the *optical theorem* as its formal solution,

$$D^{\gtrless}_{ij}(1,2) = D^{\gtrless}_{\mathrm{m},ij}(1,2) + D^{\gtrless}_{\mathrm{h},ij}(1,2), \tag{20a}$$

$$D^{\gtrless}_{\mathrm{m},ij}(1,2) = D^{\mathrm{ret}}_{ik}(1,3)P^{\gtrless}_{kl}(3,4)D^{\mathrm{adv}}_{lj}(4,2), \tag{20b}$$

where $D^{\gtrless}_{\mathrm{h}}$ are solutions of the homogeneous equation $D^{\mathrm{ret},-1}D^{\gtrless}_{\mathrm{h}} = 0$. They reflect the possibility of incident fluctuations (see Sec. III C).

Lastly, the *spectral function* $\hat{D}$ remains to be defined as

$$\hat{D}_{ij}(1,2) = D^{>}_{ij}(1,2) - D^{<}_{ij}(1,2) \tag{21}$$

with the important identity

$$\hat{D}_{ij}(1,2) = D^{\mathrm{ret}}_{ij}(1,2) - D^{\mathrm{adv}}_{ij}(1,2). \tag{22}$$

The spectral function generally splits up into a medium- and a vacuum-induced contribution according to Eq. (20a). This will be detailed in Sec. III C for slab geometry. Note that the Dyson equation promotes the Green's function identities and symmetries (see Appendix A) to the inverse GF and the polarization function such that, e.g., one has a spectral polarization function $\hat{P} = P^{>} - P^{<}$.

Now we establish the link to classical electrodynamics. We introduce the susceptibility χ of the medium such that the polarization field $\mathbf{P}$ (not to be confused with the polarization Green's function P)

$$\mathbf{P}(\mathbf{r},t) = \varepsilon_0 \int d^3\mathbf{r}'dt'\vec{\chi}(\mathbf{r},\mathbf{r}',t,t')\mathbf{E}(\mathbf{r}',t') \tag{23}$$

and $\mathbf{j}_{\mathrm{ind}} = \partial\mathbf{P}/\partial t$; as usual[17,18]

$$j_{\mathrm{ind},i}(\mathbf{r},t) = -\varepsilon_0 \int d^3\mathbf{r}'dt' \frac{\partial^2\chi_{ij}(\mathbf{r},\mathbf{r}',t,t')}{\partial t\,\partial t'}\mathbf{A}_{\mathrm{eff},j}(\mathbf{r}',t'). \tag{24}$$

With this definition, the (classical) potential equation for $\mathbf{A}_{\mathrm{eff}}(\mathbf{r},t)$ can be written as (vector component indices now omitted)

$$\left[\left(\Delta_{\mathbf{r}_1} - \frac{1}{c^2}\frac{\partial^2}{\partial t_1^2}\right)\delta(1-2) + \frac{1}{c^2}\frac{\partial^2\chi(1,2)}{\partial t_1\,\partial t_2}\right]\mathbf{A}_{\mathrm{eff}}(2) = -\mu_0\mathbf{j}_{\mathrm{ext}}(1) \tag{25}$$

and we identify $D^{0,\mathrm{ret},-1}$ as in Eq. (18) and

$$P^{\mathrm{ret}}(1,2) = -\frac{1}{c^2}\frac{\partial^2\chi(1,2)}{\partial t_1\,\partial t_2}, \tag{26}$$

finding that the retarded GF solves the classical wave propagation problem. Besides, it is often convenient to formally introduce Keldysh components for χ along the lines of the above identity, with $\chi^{\mathrm{ret}} \equiv \chi$, which then obey the GF identities and symmetries as well.

B. Photon Green's function in steady-state slab geometry

The preceding general theory will now be adapted to a specific system. We regard an isotropic medium in a steady state. It is infinitely extended in the y-z direction and has a finite thickness L in the x direction. (The generalization to anisotropic media is straightforward but not trivial.) We will consider its linear response on one hand and its emission

without external (coherent) excitation on the other hand. The first implies that Eq. (9) is to be taken at $\mathbf{A}_{\mathrm{eff}} \equiv 0$; interestingly, the second results in the same condition.

For notational simplicity, TE-polarized light propagating freely in the transverse direction is considered. Due to the cylindrical symmetry, we may choose the vector potential in z direction ($\mathbf{A}_{\mathrm{eff}} = A_{\mathrm{eff},z} =: A$). Then, potential equation (7) and the Dyson equation (11) are invariant to transverse translations and can be Fourier transformed with respect to $(y,z) \rightarrow \mathbf{q}_\parallel$. Because a steady-state system is homogeneous in time, we may also Fourier transform $(t_1 - t_2)$ dependencies to ω.

With these assumptions and transformations, the Dyson equation for the retarded GF finally reads

$$D^{\mathrm{ret},-1}(x,x',\omega,\mathbf{q}_\parallel) D^{\mathrm{ret}}(x',x'',\omega,\mathbf{q}_\parallel) = \delta(x - x'') \tag{27}$$

with

$$D^{\mathrm{ret},-1}(x,x',\omega,\mathbf{q}_\parallel) = D^{0,\mathrm{ret},-1}(x,x',\omega,\mathbf{q}_\parallel) - P^{\mathrm{ret}}(x,x',\omega,\mathbf{q}_\parallel). \tag{28}$$

Here and in what follows, the variables ω and $\mathbf{q}_\parallel$ enter the equations parametrically only and are omitted where possible. The inverse free photon GF is

$$D^{0,\mathrm{ret},-1}(x,x') = \left(\frac{\partial^2}{\partial x^2} + q_0^2 \right) \delta(x - x'). \tag{29}$$

In it, q_0 is the x component of the vacuum wave vector

$$\mathbf{q} = \frac{\omega + \mathrm{i}\delta}{c} \mathbf{e}_q = q_0 \mathbf{e}_x + \mathbf{q}_\parallel, \tag{30}$$

in which the infinitesimal imaginary contribution assures causality. The angle of incidence α then is determined by $q_0 = |\mathbf{q}| \sin \alpha$. P^{ret} is related to the susceptibility as

$$P^{\mathrm{ret}}(x,x') = -\frac{\omega^2}{c^2} \chi(x,x'). \tag{31}$$

This simplified structure is quasi-one-dimensional but still allows to exactly include SD as well as spatial inhomogeneity in the x direction. Several useful symmetry relations arise, which are listed in Appendix A.

C. Separation of vacuum- and medium-induced contributions

The kinetic Dyson equation (19) is an inhomogeneous integrodifferential equation for $D^{\gtrless}$ to which arbitrary homogeneous solutions $D_h^{\gtrless}$ may be added. The spectral function $\hat{D}$ [Eq. (21)] can be constructed as the difference of either $D^>$ and $D^<$ or D^{ret} and D^{adv}. The latter both are uniquely defined through the radiation condition. Consequently, the difference $D^> - D^<$ is fixed too. It can be written as

$$\hat{D} = D^{\mathrm{ret}} \hat{P} D^{\mathrm{adv}} + D_h^> - D_h^< = \hat{D}_m + \hat{D}_v. \tag{32}$$

The spectral function thus is split up into a contribution caused by the medium via P, $\hat{D}_m$, and one which cannot be attributed to the medium, $\hat{D}_v$.

In order to express $\hat{D}_v$ by known functions, we may construct the expression $D^{\mathrm{ret},-1} \hat{D} D^{\mathrm{adv},-1}$ and transform it as follows:

$$\begin{aligned} D^{\mathrm{ret},-1} \hat{D} D^{\mathrm{adv},-1} &= \hat{P} + D^{\mathrm{ret},-1} \hat{D}_v D^{\mathrm{adv},-1} \Leftrightarrow D^{\mathrm{adv},-1} - D^{\mathrm{ret},-1} \\ &= \hat{P} + D^{\mathrm{ret},-1} \hat{D}_v D^{\mathrm{adv},-1} \Leftrightarrow D^{0,\mathrm{adv},-1} - D^{0,\mathrm{ret},-1} \\ &= D^{\mathrm{ret},-1} \hat{D}_v D^{\mathrm{adv},-1}. \end{aligned} \tag{33}$$

With the last step, the medium contribution has been eliminated. Using Eq. (29) and GF symmetries on the left-hand side (LHS), we find

$$D^{0,\mathrm{adv},-1}(x,x') - D^{0,\mathrm{ret},-1}(x,x') = -\frac{4\mathrm{i}\delta\omega}{c^2} \delta(x - x') \tag{34}$$

and thus have by multiplication of Eq. (33) by $D^{\mathrm{ret}}, D^{\mathrm{adv}}$

$$\hat{D}_v(x,x') = -\mathrm{i}\delta \frac{4\omega}{c^2} \int dx_2 D^{\mathrm{ret}}(x,x_2) D^{\mathrm{adv}}(x_2,x'), \tag{35}$$

an expression whose properties allow for interesting further considerations.

Note that $\hat{D}_v$ contains the infinitesimal prefactor δ, which is exactly compensated by the improper integral in Eq. (35) being $\propto 1/\delta$. Also, $\hat{D}_v$ is a solution of the homogeneous Dyson equation (19), which follows by applying $D^{\mathrm{ret},-1}$ on it,

$$D^{\mathrm{ret},-1} \hat{D}_v = -\mathrm{i}\delta \frac{4\omega}{c^2} D^{\mathrm{adv}} \overset{\delta \rightarrow 0}{\rightarrow} 0. \tag{36}$$

So $D_h^{\gtrless}$ must be proportional to $\hat{D}_v$; i.e., $D_h^{\gtrless} = n^{\gtrless} \hat{D}_v$ with prefactors $n^{\gtrless}$. Their difference is fixed by Eq. (32) to $n^< = n^> - 1$. Apart from that, $n^{\gtrless}$ may be arbitrary since a homogeneous solution cannot be normalized.

Since $\hat{D}_v$ is a spectral function, its prefactor can be interpreted as a mode occupation number.[14] It is composed of the correlators $D_h^{\gtrless}$, which remain even in the absence of the medium [$P \rightarrow 0$ in Eq. (20b)] and thus must represent fluctuations[14] of the vacuum. In other words, $n(\omega,\mathbf{q}_\parallel) = n^<(\omega,\mathbf{q}_\parallel)$ describes the distribution of fluctuations incident on the slab from the outside [see also the discussion of Eq. (61)]. Finally, the optical theorem reads

$$D^{\gtrless} = D_m^{\gtrless} + n^{\gtrless} \hat{D}_v. \tag{37}$$

In the following theory, the splitting plays an important role. We will call $\hat{D}_v$ the *vacuum-induced* contribution, which will be seen to enter the relations for dissipation and emission alone, while the *medium-induced* contribution $\hat{D}_m$ exactly cancels out. There are other options for splitting the spectral function. Most important, the spectral function of the *pure vacuum*

$$\hat{D}^0 = D^{0,\mathrm{ret}} - D^{0,\mathrm{adv}}, \tag{38}$$

in slab geometry

$$\hat{D}^0(x,x',\omega,\mathbf{q}_\parallel) = \frac{1}{2\mathrm{i}q_0} \cos[q_0(x - x')], \tag{39}$$

can be separated from $\hat{D}$, but it is not to be confused with $\hat{D}_v$. Only the splitting as shown in Eq. (32) separates clearly the contributions involved in emission and absorption from those that cancel out.

During the preparation of this paper, one of us (K.H.) was able to prove that this splitting does not depend on a certain geometry, medium, or temporal homogeneity but rather is an exact universal property of the photon Green's functions. The proof, which is presented in Ref. 19, takes a slightly different approach and might be instructive to the reader too.

D. Solution structure for the vector potential

In order to describe a traditional transmission-reflection experiment, the external source on the right-hand side of Eq. (25) is to be put zero and instead an external wave incoming from left or right is assumed. Consequently, there are two linearly independent solutions for incidence from left or right.

The thickness L of the slab is defined such that any polarization and any Keldysh component of the polarization function vanish for $|x|>L/2$. We then have the vacuum solution

$$A(x)=\begin{cases} e^{iq_0x}+re^{-iq_0x}, & x<-L/2 \\ te^{iq_0x}, & x>L/2 \end{cases} \tag{40}$$

in the forward propagating case and a solution $A(-x)$ for the backward propagating case. It describes incident, reflected, and transmitted light as plane waves. The amplitude of the incident wave is chosen as unity, so that r,t are the reflection and transmission coefficients.

These solutions are fixed by their asymptotics and there is no need to impose any further boundary conditions on them (even not Maxwell's) since the polarization of the medium increases continuously in the transition region from vacuum to medium and, consequently, the solutions of Eq. (25) evolve continuously too from the asymptotic ones (compare also the discussion in Ref. 20). Only if one assumes an abrupt switch of the polarization at the surface, one has to make sure the continuity of the solutions of Eq. (25) by imposing Maxwell's boundary conditions.

Inside the slab, an analytical solution cannot generally be given. It has to be constructed from the retarded GF or with the help of the constitutive relation (23). For a spatially homogeneous medium, the susceptibility function can be transformed to $\chi(\mathbf{q},\omega)$, and the solutions inside are the *polariton solutions*

$$A(x)=\sum_i A_i^+ \exp(iq_{x,i}x)+A_i^- \exp(-iq_{x,i}x), \tag{41}$$

which obey the *polariton dispersion*

$$\mathbf{q}_i^2=\frac{\omega^2}{c^2}[1+\chi(\mathbf{q}_i,\omega)]=q_{x,i}^2+\mathbf{q}_\parallel^2. \tag{42}$$

Maxwell's boundary conditions determine the system if only one mode is present. In the presence of additional polariton modes, additional boundary conditions (ABCs) have to be imposed. Several possibilities with a higher or lower degree of arbitrariness exist and are subjected to intense debate over the last decades. Most of the ABCs can be reproduced by *generalized (Pekar's) ABCs*.[17,18]

Using further $\chi(\mathbf{q},\omega)\approx\chi(0,\omega)$ allows to reproduce the results of Ref. 5 but also means neglecting the effect of spatial dispersion. In principle, only an infinitely extended ("bulk") medium is spatially homogeneous, so these two steps are approximations. However, the present theory exactly includes inhomogeneities in χ.

E. Energy flow and conservation

Poynting's theorem is a suitable starting point for energy flow and conservation considerations.[17] Here, the electromagnetic energy flow between medium and vacuum is of interest. The time derivative of the energy density $\partial U_e/\partial t$ vanishes in the steady state, and due to the transversal translation invariance in slab geometry, energy can only flow in the x direction. After integration over the medium boundaries, the theorem yields for the Poynting energy flux vector $\mathbf{S}=(S,0,0)$

$$S(L/2)-S(-L/2)=-\int_{-L/2}^{L/2} dx\, j(x)E(x), \tag{43}$$

where $W(x)=j(x)E(x)$ is the density of dissipated energy (heat). Both sides are $\omega,\mathbf{q}_\parallel$ integrals over spectrally and directionally resolved quantities s,w which will be introduced later.

Classical fields and coherent absorption

At first, Poynting's theorem (43) will be addressed for average fields (classical light). Therefore, a monochromatic wave of frequency ω_0 incident in the direction $\mathbf{q}_{\parallel,0}$ is assumed; i.e.,

$$A_{\mathrm{mc}}(x,\omega,\mathbf{q}_\parallel)=\frac{1}{2}[A_0(x,\omega_0,\mathbf{q}_{\parallel,0})\delta(\omega-\omega_0)\delta_{\mathbf{q}_\parallel,\mathbf{q}_{\parallel,0}} + A_0^*(x,\omega_0,\mathbf{q}_{\parallel,0})\delta(\omega+\omega_0)\delta_{\mathbf{q}_\parallel,-\mathbf{q}_{\parallel,0}}]. \tag{44}$$

This construction assures that $A_{\mathrm{mc}}(\mathbf{r},t)$ is real. Evaluating, on one hand, the Poynting vector

$$S(x,t)=\frac{1}{\mu_0}[\mathbf{E}(x,t)\times\mathbf{B}(x,t)]\big|_x=-\frac{1}{\mu_0}\frac{\partial A(x,t)}{\partial t}\frac{\partial A(x,t)}{\partial x} \tag{45}$$

with the vacuum solution for the vector potential [Eq. (40)] and, on the other hand, the dissipation inside the medium

$$W(x,t)=j(x,t)E(x,t)=-\frac{\partial P(x,t)}{\partial t}\frac{\partial A(x,t)}{\partial t} \tag{46}$$

with P as the polarization field [Eq. (23)], one finds that the static parts of these quantities obey the identity

$$1-|r|^2-|t|^2=a=\frac{\omega^2}{q_0c^2}\,\mathrm{Im}\int_{-L/2}^{L/2} dx dx' A^*(x)\chi(x,x')A(x') \tag{47}$$

for any $\omega,\mathbf{q}_\parallel$. The LHS difference of normalized incoming light intensity and transmittivity and reflectivity is just the absorptivity a of the medium.

This identity thus relates the nonlocal susceptibility $\chi(x,x')$ (whose imaginary part is called "microscopic ab-

sorption" in media where $\chi(x,x')=\chi(x',x)$) and the vector potential inside the medium to its absorptivity. It is an energy conservation equation and can serve as a hard criterion for theoretical models and numerical simulations. Here, the reflected and transmitted light may be regarded as the intensity re-emitted coherently to the incoming light and is to be contrasted with the *incoherent* (or *correlated*) emission, which will be addressed below.

F. Green's function representation of the incoherent energy flow

In this subsection, we will derive the Green's function representation of the constituents in Poynting's theorem, transform them to slab geometry, and resolve them spectrally and directionally. Correlated emission is a quantum-mechanical phenomenon and it is defined as the one without external sources, i.e., vanishing effective fields. The field operators needed in Poynting's theorem (43) do not commute, so symmetrized operators $\hat{X}\hat{Y}|_{\mathrm{sym}}=(\hat{X}\hat{Y}+\hat{Y}\hat{X})/2$ have to be used.

First, the Poynting vector in symmetrized form can be expressed straightforward in terms of the vector potential $\hat{A}$ according to Ref. 5 as

$$\begin{aligned}\hat{S}_i(1) &= \frac{1}{\mu_0}[\hat{\mathbf{E}}(1)\times\hat{\mathbf{B}}(2)]_{i,\mathrm{sym}}|_{1=2}\\ &= \frac{1}{2\mu_0}\frac{\partial}{\partial t_1}\{\nabla_j(2)[\hat{A}_j(1)\hat{A}_i(2)+\hat{A}_i(2)\hat{A}_j(1)]\\ &\quad -\nabla_i(2)[\hat{A}_j(2)\hat{A}_j(1)+\hat{A}_j(1)\hat{A}_j(2)]\}|_{1=2}. \end{aligned} \tag{48}$$

Then, its expectation value $\langle\hat{S}_i(1)\rangle$ can be easily transformed to GFs as follows:[5]

$$\begin{aligned}\langle\hat{S}_i(1)\rangle &= \frac{i\hbar}{2\mu_0}\frac{\partial}{\partial t_1}\{\nabla_j(2)[D^{>}_{ji}(1,2)+D^{<}_{ji}(1,2)]\\ &\quad -\nabla_i(2)[D^{>}_{jj}(1,2)+D^{<}_{jj}(1,2)]\}|_{1=2}. \end{aligned} \tag{49}$$

This general expression can be simplified for the slab geometry. For TE-polarized light, only the zz component of $D^{\gtrless}$ and the x component of $\mathbf{S}$ are nonzero, so only the second term can contribute. After Fourier transformations $(t_1-t_2)\to\omega$ and $(\mathbf{r}_{\parallel,1}-\mathbf{r}_{\parallel,2})\to\mathbf{q}_{\parallel}$, the time derivative can be trivially taken. Finally, negative frequencies are mirrored to positive values. The result is

$$S(x)=\int_0^\infty\frac{d\omega}{2\pi}\hbar\omega\int\frac{d^2\mathbf{q}_{\parallel}}{4\pi^2}s(x,\omega,\mathbf{q}_{\parallel}), \tag{50}$$

$$s(x,\omega,\mathbf{q}_{\parallel})=-\frac{1}{\mu_0}\left\{\frac{\partial}{\partial x_1}\mathrm{Re}[D^{>}(x,x_1)+D^{<}(x,x_1)]\right\}_{x_1\to x} \tag{51}$$

with parameters $\omega,\mathbf{q}_{\parallel}$ omitted on the right.

The formulation of the symmetrized dissipation $\hat{W}=(\hat{\mathbf{j}}\cdot\hat{\mathbf{E}})_{\mathrm{sym}}$ in terms of PGFs, which results in

$$\int dx W(x)=\int_0^\infty\frac{d\omega}{2\pi}\hbar\omega\int\frac{d^2\mathbf{q}_{\parallel}}{4\pi^2}w(\omega,\mathbf{q}_{\parallel}), \tag{52}$$

$$\begin{aligned}w(\omega,\mathbf{q}_{\parallel}) &= \int dx_1\int dx_2[n^{>}P^{<}(x_1,x_2)\\ &\quad -n^{<}P^{>}(x_1,x_2)]\hat{D}_v(x_2,x_1)\end{aligned} \tag{53}$$

is lengthy and more difficult. Details are given in Appendix B. Note that the dissipation contains no contribution from $\hat{D}_m$.

Both quantities decompose into spectrally and directionally resolved quantities, which can be analyzed separately. Now that the energy flow is properly formulated in GFs, further evaluation requires the knowledge of the retarded Green's function, to which Sec. III G is devoted.

G. Retarded photon Green's function

For the pure vacuum case, $D^{\mathrm{ret}}(x,x')=\frac{1}{2iq_0}\exp(iq_0|x-x'|)$ solves Eq. (27). Its physical interpretation is clear: It is the wave emitted by a unit source at x' which propagates into both directions and is observed at x.

In the presence of the medium, this interpretation is still valid but the solution now is determined by the full $D^{\mathrm{ret},-1}$ and cannot generally be given analytically. However, we will see that a full analytical solution is not needed and we may confine ourselves to the case $|x'|>L/2$, i.e., sources outside the medium.

With this restriction, D^{ret} can be given in terms of the piecewise defined vector potential [Eq. (40)] as

$$\begin{aligned}D^{\mathrm{ret}}(x,x') &= \frac{1}{2iq_0t}[\Theta(x-x')A(x)A(-x')\\ &\quad +\Theta(x'-x)A(x')A(-x)].\end{aligned} \tag{54}$$

Knowing D^{ret}, $\hat{D}_v$ can be expressed in terms of A as well. The improper integral in its definition [Eq. (35)] contains a $1/\delta$ divergency, which is compensated by the δ prefactor. Thus, one may leave out the unknown but finite contribution of the medium ($|x_2|<L/2$) without changing the integral value. Some straightforward calculation yields

$$\hat{D}_v(x,x')=\frac{1}{2iq_0}[A(x)A^*(x')+A(-x)A^*(-x')]. \tag{55}$$

This result has already been shown in Ref. 4 neglecting spatial dispersion, but it is derived here under full consideration of spatial inhomogeneity in the x direction.

Furthermore, for the medium contribution to the spectral function, $\hat{D}_m$ follows from Eq. (32) for any $|x|>L/2, |x'|>L/2$

$$\hat{D}_m(x,x')=\frac{a}{2iq_0}\exp[iq_0(x-x')], \tag{56}$$

where a is the absorptivity defined in Eq. (47). In the case that the susceptibility is used in the bulk approximation, it can be shown that Eqs. (54) and (56) are valid without spatial restriction to x or x'.

H. Dissipation as balance of generation and recombination, internal and external photons

Using Eq. (55) in Eq. (52) and defining the global generation and recombination rates

$$\mathfrak{P}^{\gtrless}(\omega,\mathbf{q}_\parallel) = \int dx \int dx' A^*(x) P^{\gtrless}(x,x') A(x') = \mathrm{i}q_0 \int dx \int dx' P^{\gtrless}(x,x') \hat{D}_v(x',x) \tag{57}$$

yields

$$w(\omega,\mathbf{q}_\parallel) = \frac{1}{\mathrm{i}q_0}[n^<\mathfrak{P}^> - n^>\mathfrak{P}^<]. \tag{58}$$

We see the dissipation w here as the difference of

(i) an optical excitation of the medium $\mathrm{i}\mathfrak{P}^>$ stimulated by incident photons (thus proportional to $n^<=n$) and

(ii) in view of $n^>=n+1$, recombination $\mathrm{i}\mathfrak{P}^<$ stimulated by incident photons ($\propto n$) plus spontaneous recombination or emission ($\propto 1$).

The "microscopic" generation and recombination rates $P^{\gtrless}(x,x')$ are related to the microscopic absorption (susceptibility) through $P^>-P^<=\hat{P}=P^{\mathrm{ret}}-P^{\mathrm{adv}}$ and Eq. (31) just as the global rates $\mathfrak{P}^{\gtrless}$ are related to the classical absorptivity (47),

$$\mathrm{i}\hat{\mathfrak{P}}(\omega,\mathbf{q}_\parallel) = 2q_0 a(\omega,\mathbf{q}_\parallel). \tag{59}$$

The ratio of global generation and recombination to the global absorption defines a distribution $b=b^<$

$$b^{\gtrless}(\omega,\mathbf{q}_\parallel) = \frac{\mathfrak{P}^{\gtrless}(\omega,\mathbf{q}_\parallel)}{\hat{\mathfrak{P}}(\omega,\mathbf{q}_\parallel)}, \tag{60}$$

which obeys $b^<=b^>-1$ due to the identity $\hat{\mathfrak{P}}=\mathfrak{P}^>-\mathfrak{P}^<$. It characterizes globally the distribution of medium-induced optical excitations (e.g., polaritons in semiconductors) over the absorption or gain spectrum (distribution of "internal photons").

Notably, while the balance of generation and recombination stimulated by the external photon bath gives the dissipation w in Eq. (58), the same stimulated by internal photons cancels exactly; $b^>\mathfrak{P}^<-b^<\mathfrak{P}^>=0$. In other words, spontaneous and stimulated re-emission and reabsorption always cancel in steady state. Furthermore, also the medium contribution to the spectral function $\hat{D}_m$ cancels out in the dissipation.

With the above definition of b inserted, the optical theorem [Eq. (37)] takes the form

$$D^{\gtrless} = b^{\gtrless}\hat{D}_m + n^{\gtrless}\hat{D}_v, \tag{61}$$

where the spatial restrictions of Eq. (56) apply. This form shows that the medium- and vacuum-induced field fluctuations are weighted by the distributions of internal and external photons, respectively. Thus, neither internal photon stimulations nor medium-induced field fluctuations contribute to the energy transport between the medium and the environment.

I. Nonequilibrium energy flow

In the case that emission with vanishing external fields is regarded, the energy flow will be equal at both surface sides of the slab and Eq. (43) gives the energy flow law referred to in Sec. I,

$$s(L/2,\omega,\mathbf{q}_\parallel) = -\frac{1}{2}w(\omega,\mathbf{q}_\parallel) = [b(\omega,\mathbf{q}_\parallel) - n(\omega,\mathbf{q}_\parallel)]a(\omega,\mathbf{q}_\parallel), \tag{62}$$

in which the spectrally and angular resolved energy flux s is composed of emission $s_e=ba$ and absorption $s_a=-na$. It will be discussed in detail in Sec. IV. The density of the total-energy flux, which propagates only in the x direction, is given by the integral

$$S(L/2) = \int \frac{d\omega}{2\pi}\hbar\omega \int \frac{d^2\mathbf{q}_\parallel}{(2\pi)^2} s(L/2,\omega,\mathbf{q}_\parallel). \tag{63}$$

IV. DISCUSSION

A. Emission and absorption contributions to the energy flux

In Eq. (62), $s_a=-na$ describes an energy flux as the response of the medium to (and stimulated by) the given nonequilibrium distribution n of external photons. In contrast, $s_e=ba=\mathrm{i}\mathfrak{P}^</2q_0$ describes the emission of medium-induced light as the response of the medium to vacuum fluctuations or emission due to spontaneous recombination.

In the case of absorption ($a>0$) the contribution of s_a is negative and that of s_e positive. In the presence of gain ($a<0$), however, s_a becomes the positive contribution of amplified vacuum-induced light, while b changes sign ($b=\mathrm{i}\mathfrak{P}^</2q_0a<0$) so that s_e stays positive.

If the externally given incoherent radiation field incident from the outside is strong, i.e., for $n \gg b$, measuring the energy flow $s \approx s_a$ would provide the same information as a classical (coherent) reflection-transmission experiment, namely, the absorptivity $a=s_a/n$. In the opposite case, $b \gg n \to 0$, the pure emission s_e into the vacuum can be measured, and the nonequilibrium distribution b is accessible to direct observation in experiments measuring simultaneously the (incoherent) emission and the linear coherent absorptivity, i.e., transmittivity and reflectivity. Notably, for both coherent and incoherent light, the absorptivity involved is the same. Otherwise, the emission could be obtained by rigorous calculation of $\mathrm{i}\mathfrak{P}^<$ from the particle Green's functions of the interacting system of light and matter.

B. Angle dependency

We introduce the frequency-resolved angle-integrated energy flux $\bar{s}(\omega)$

$$\bar{s}(\omega) = \int_{-\omega/c}^{\omega/c} \frac{d^2\mathbf{q}_\parallel}{(2\pi)^2} s(L/2,\omega,\mathbf{q}_\parallel), \tag{64}$$

to which different propagation directions contribute according to Eq. (30) even though there is no resulting energy

transport in the y-z direction. Because the x component of $\mathbf{q}$, q_0, must be positive, $\mathbf{q}_\parallel^2 \leq \omega^2/c^2$.

For some insight into the effects of this integration, we consider the bulk approximation for χ with the corresponding dispersion relation and vector potential [Eqs. (41) and (42)]. Then, a change in $\mathbf{q}_\parallel$ at fixed ω will result in a change in the internal wave vector in x direction q_x. This affects the Fabry-Perot resonances (FPRs) which occur roughly if

$$\mathrm{Re}\, q_x = N\frac{\pi}{L} \tag{65}$$

is met with an integer N. This will be discussed further in Sec. V A in an example case.

Real-world semiconductors are not infinitely extended, but this theory relies on the simplifications introduced by the slab geometry, and an exact analytical treatment of the finite slab has not yet been achieved. The boundary conditions in the y and z directions would be extremely difficult to handle.

As an approximation for a finite slab, the $\mathbf{q}_\parallel$ integral could be limited to its acceptance angle, and one may additionally approximate $\mathbf{q}_\parallel = 0$ under the integral if this angle is small enough. In lasers, it is usually sought to narrow the solid angle of the emission by cavity design.[4]

C. Quasiequilibrium

If the matter subsystem can be prepared in a way that it is in a thermodynamic (quasi)equilibrium state, a special fundamental property of the Green's functions, the *Kubo-Martin-Schwinger relation*, holds[1,2,13,21] for the polarization function

$$P^<(\omega) = \exp\left[-\frac{1}{k_B T}(\hbar\omega - \mu)\right] P^>(\omega). \tag{66}$$

Writing down $\hat{\mathfrak{P}}$ under this condition, one easily sees that the distribution $b(\omega, \mathbf{q}_\parallel)$ must develop into a Bose function and become independent of $\mathbf{q}_\parallel$ if quasiequilibrium is reached. The chemical potential μ, which enters the relation through the statistical operator of the grand canonical ensemble, then acts as a measure of the excitation of the system, starting from $\mu = 0$ for complete thermal equilibrium and increasing to $\mu > 0$ for an excited quasiequilibrium state. While the external photon bath obviously can be expected to be Bose distributed in the equilibrium case, it is nontrivial that this is always the case for the medium-induced optical excitations regardless of the (fermionic) matter subsystem they are coupled to.

In an excited semiconductor, the crossover from absorption $a > 0$ to gain $a < 0$ appears independently of $\mathbf{q}_\parallel$ at $\hbar\omega = \mu$, where the singularity in b is compensated by the zero in a. Hence, expanding b^{-1} and a at $\hbar\omega = \mu$ yields that the emission s_e stays finite at the crossover and is given by the slope of the absorption according to $s_e(\mu, \mathbf{q}_\parallel) = k_B T \{\partial a(\omega, \mathbf{q}_\parallel)/\partial\omega\}_{\hbar\omega=\mu}$. Since both a and b switch their signs, the emission stays positive for any frequency as it should be. Measuring b via s_e and $a = 1 - |r|^2 - |t|^2$ would enable to check whether quasiequilibrium is realized. If so, the chemical potential μ is fixed through the crossover point and, after that, the temperature and excitation density can be obtained directly from experimental data (see Sec. V D).

D. Relation to Kirchhoff and Planck laws

The following derivation will show that the nonequilibrium energy flow law [Eq. (62)] and the Kirchhoff law become equivalent in thermal equilibrium and that the Bose distribution b then corresponds to the Planck formula for the spectral radiance. The total energy of Bose-distributed free photons with wave vector $\mathbf{q}$ is

$$E = \sum_{\mathbf{q}} \hbar c q n_q = \sum_{\mathbf{q}} \frac{\hbar c q}{\exp\left(\frac{\hbar c q}{k_B T}\right) - 1}. \tag{67}$$

The corresponding energy density can be given resolved for wave vectors or frequencies,

$$\frac{E}{V} = \int \frac{d^3\mathbf{q}}{(2\pi)^3} u(q), \quad u(q) = \frac{\hbar c q}{\exp\left(\frac{\hbar c q}{k_B T}\right) - 1},$$

$$\frac{E}{V} = \int d\omega\, u(\omega), \quad u(\omega) = \frac{\hbar\omega^3}{2\pi^2 c^3} \frac{1}{\exp\left(\frac{\hbar\omega}{k_B T}\right) - 1} \tag{68}$$

with the latter being Planck's spectral radiance divided by c.

The energy flux of a single photon is the product of its velocity c and the unit wave vector $\mathbf{q}/q$, so the entire photon energy flux density is

$$\mathbf{S} = \int \frac{d^3\mathbf{q}}{(2\pi)^3} \frac{\mathbf{q} c}{q} u(q). \tag{69}$$

We express the infinitesimal volume element in a form suitable for slab geometry,

$$d^3\mathbf{q} = d^2\mathbf{q}_\parallel dq_0 = d^2\mathbf{q}_\parallel d\omega \frac{\omega}{c^2} \frac{1}{q_0(\omega, \mathbf{q}_\parallel)} \tag{70}$$

and obtain the energy flux density of the blackbody (cavity) radiation in x direction,

$$S_x = \int \frac{d\omega}{2\pi} \hbar\omega \int \frac{d^2\mathbf{q}_\parallel}{(2\pi)^2} s(\omega, \mathbf{q}_\parallel), \tag{71}$$

where $s = b$ is a Bose function with $\mu = 0$. According to Eq. (62), it is equivalent to the energy flux emitted by an ideally absorbing slab ($a \equiv 1$) in complete thermal equilibrium. In the *Hohlraum* case, i.e., if body and environment are in radiative equilibrium, $n \equiv b$ and Kirchhoff's law is met as the limiting case with the proportionality factor of the emission corresponding to Planck's spectral radiance formula.

E. Low-temperature behavior and quantum condensation

For $T \to 0$, the Bose function degenerates to a step function. The emission $s_e(\omega, \mathbf{q}_\parallel) \to -\Theta(\mu - \hbar\omega) a(\omega, \mathbf{q}_\parallel)$ vanishes completely in the absorption region $\hbar\omega > \mu$ and reflects exactly the gain $-a$ in the gain region $\hbar\omega < \mu$.

The theory given above needs to be supplemented if effects of quantum condensation occur. As such, the crossover from Bose-Einstein condensation of excitons at moderate ex-

citation to the one of Cooper-type electron-hole pairs at high excitation has been addressed.[22,23] A recently presented approach[24,25] allows to analyze the consequences of quantum condensation for emission and absorption spectra. Some basic features should be commented on here.

If quantum condensation occurs, an anomalous contribution will appear in addition to the normal generation $i\mathfrak{P}^{>}$ and recombination $i\mathfrak{P}^{<}$ considered above via[25]

$$P^{\gtrless}(x,x') \to P^{\gtrless}(x,x') + P_{\mathrm{cond}}(x)\delta_{\mathbf{q}_{\parallel},0}\delta(x-x')\delta(\hbar\omega-\mu). \tag{72}$$

The strength P_{cond} is determined by the fraction of quasiparticles in the condensate. Since it appears identically in both the generation and the recombination, its influence cancels in the classical absorptivity a according to Eqs. (47) and (31).

Consequently, those effects will not appear directly in classical absorption experiments, where at best they show up as smooth changes in the spectral shape of the absorptivity a. However, in the emission $s_e = i\mathfrak{P}^{<}/2q_0$, an additional sharp peak at $\hbar\omega=\mu$, whose strength is $\propto \int dx P_{\mathrm{cond}}(x)|A(x)|^2$, would give evidence for a condensate since the normal part of the emission just at this frequency tends toward zero for $T \to 0$.

V. APPLICATIONS

In order to illustrate the theory given above, we consider single-layer zinc selenide (ZnSe) slabs and calculate their absorption and emission spectra as well as mode densities at different levels of excitation and a temperature of 77 K. We describe their electromagnetic properties in the spectral region from the excitonic heavy-hole resonance at 2806 meV up to the band gap at 2827 meV by appropriate susceptibility functions for the bulk matter, which were originally worked out for Ref. 26.

A susceptibility function for a nonexcited ZnSe medium was constructed in the *oscillator model* with parameters (resonance energy, oscillator strength, and damping) fitted to experimental data. Susceptibilities for media at different levels of excitation, i.e., different densities of excited carriers n_e, were calculated solving the *semiconductor Bloch equations*. In the latter calculations, the dynamically screened Coulomb potential was used in the Lindhard formula approximation, and phase-space filling as well as Hartree-Fock renormalization is fully covered. The resulting susceptibilities reproduce advanced features such as higher exciton resonances, resonance broadening and shift, band-gap shrinkage, and optical gain.

The imaginary parts of all these susceptibilities are presented in Fig. 1. The dashed line corresponds to the nonexcited case. With increasing carrier density, the exciton peak is damped and broadened. For the highest excitation density, optical gain appears. The crossover from gain to absorption is at $\hbar\omega=2807$ meV and the maximum gain is -0.17.

A. Absorption spectra

The absorptivity can be calculated from Eq. (47) if amplitudes and phases of the light modes inside or outside the slab are known. These are fixed by Maxwell's boundary conditions, i.e., a continuous transition of the fields and their first derivatives at the medium surfaces.

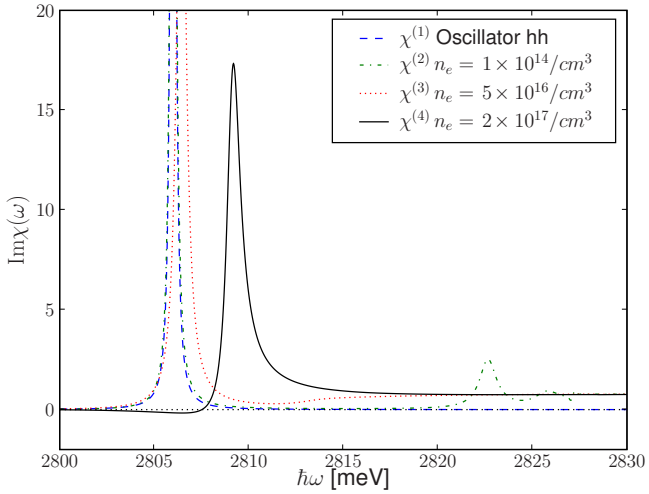

FIG. 1. (Color online) Imaginary part of susceptibilities χ in a ZnSe slab at $T=77$ K for different levels of excitation. $\chi^{(4)}$ features a crossover from gain to absorption at $\hbar\omega=2807$ meV and a maximum gain of -0.17. The maxima of Im $\chi^{(1)-(4)}$ are 143.3, 109.2, 37.3, and 17.3. In $\chi^{(2)}$, excited exciton state resonances and the band gap are visible.

As a macroscopic description of the system, the *dielectric approximation*[17,20]

$$\chi(x,x',\omega) = \Theta(|x| < L/2)\chi(x-x',\omega)\Theta(|x'| < L/2) \tag{73}$$

may be employed for the susceptibility, i.e., that of a spatially homogeneous medium cut off at the medium boundaries by step functions. One may then use the susceptibility in the bulk approximation $\chi(\mathbf{q},\omega)$. The corresponding dispersion relation and solutions for the vector potential are given in Eqs. (41) and (42). In a further approximation, spatial dispersion may be neglected by taking $\chi(\mathbf{q}=0,\omega) = \chi(\omega)$.

Figure 2 compares the absorptivity of a 500 nm ZnSe slab with and without spatial dispersion. The polariton solutions result in dense and fine FPR structures in the absorptivity, so it is important for any quantitative analysis to consider spatial dispersion. In both cases, the resonances appear very dense in the spectral range of the exciton binding energy, where Re χ features a sweep. Figure 3(a) shows the angle dependence with spatial dispersion. Resonances shift with increasing angle if χ is flat in the respective energy range but shift only weakly close to the exciton resonance.

The longer the slab, the more Fabry-Perot resonances will occur. Those induced by spatial dispersion wash out with increasing length. In the following, spatial dispersion will be neglected for the excited slabs for simplicity and a more qualitative discussion.

The corresponding susceptibilities $\chi^{(2)-(4)}$ have been obtained by an extensive numerical evaluation of the semiconductor Bloch equations with many-particle effects, namely, gain shift, line broadening and shifting, and Pauli blocking. They reproduce spectral features such as the hydrogen series of exciton states, the band gap, and gain in the absorptivity

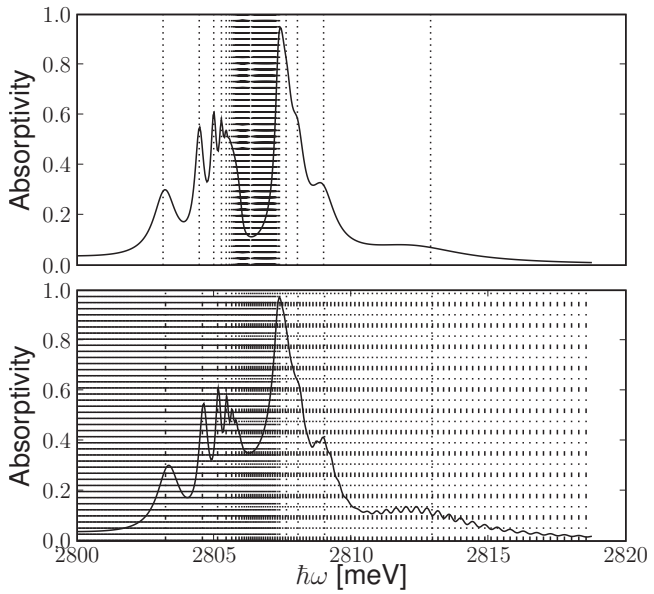

FIG. 2. Absorptivity a for normal incidence ($\mathbf{q}_\parallel=0$) as a function of energy $\hbar\omega$ for a nonexcited ZnSe slab of thickness $L=500$ nm calculated with $\chi=\chi^{(1)}$. Top: neglecting spatial dispersion. Dotted vertical lines mark Fabry-Perot resonances for the resulting single mode. Bottom: with spatial dispersion. Additional resonances appear. Dash-dotted vertical lines mark resonances for polariton mode q_1 and dotted lines for q_2.

plots in Figs. 3(b) and 3(c). In the presence of gain, the absorptivity develops pronounced negative peaks, with $|a| \gg 1$ for any angle but strongly increases when the FPR condition is approached [note the logarithmic scale in Fig. 3(c)], and thus gives rise to strong stimulated light amplification in the emission $s_e=ba$.

B. Quasiequilibrium emission and lasing

In order to calculate the emission from a material with known absorptivity, only the distribution b has to be known. It has in principle to be rigorously calculated from the particle GFs. Here, we will assume the matter subsystem to be in quasiequilibrium and make use of the fact that b becomes a Bose function in this case. Temperature T and chemical potential μ have to be chosen according to the excitation. Because b then is independent of $\mathbf{q}_\parallel$, the angle-integrated emission according to Eq. (64) can be written as

$$\bar{s}_e(\omega) = b(\mu,T)\bar{a}(\omega), \tag{74}$$

$$\bar{a}(\omega) = \int_{-\omega/c}^{\omega/c} \frac{d^2\mathbf{q}_\parallel}{(2\pi)^2} a(\omega,\mathbf{q}_\parallel). \tag{75}$$

The angle-integrated absorptivity $\bar{a}$ for a weakly excited slab (with $\chi=\chi^{(2)}$, corresponding to a carrier density of 10^{14} cm^{-3}) is shown in Fig. 4 in arbitrary units (a.u.) together with $a(\omega,\mathbf{q}_\parallel)$ for several angles of incidence. The integration smoothes the FPR structures. By multiplication of an appropriate Bose function ($\mu\approx 2757$ meV and $T=77$ K), the spectrally resolved quasiequilibrium emission $\bar{s}_e$ follows.

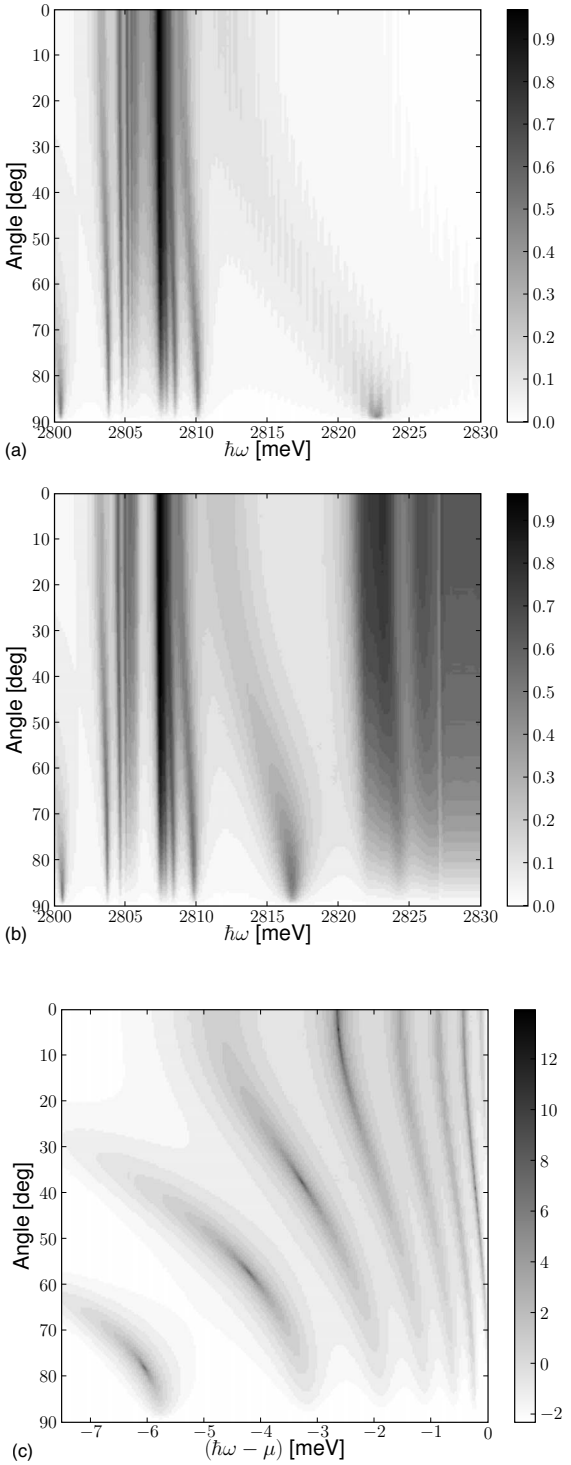

FIG. 3. Absorptivity a as a function of energy $\hbar\omega$ and angle of incidence in ZnSe slabs at different levels of excitation. (a) Absorptivity a for a non-excited slab, $L=500$ nm, $\chi^{(1)}(\mathbf{q},\omega)$, i.e., including spatial dispersion. Resonances at energies where $\chi(\omega)$ is flat shift strongly with increasing angle. To the contrary, resonances at sweeps in χ shift only little. (b) As above, but for a weakly excited slab, $\chi^{(2)}(\mathbf{q}=0,\omega)$. Higher exciton state resonances and the band gap are visible. (c) Logarithm of the gain ($\log(-a)$) below the crossover ($\hbar\omega<\mu=2807$ meV) for the strongly excited case, $L=2.5$ μm, $\chi^{(4)}(\mathbf{q}=0,\omega)$. Build-up of very pronounced peaks at certain angles as FPR condition is approached.

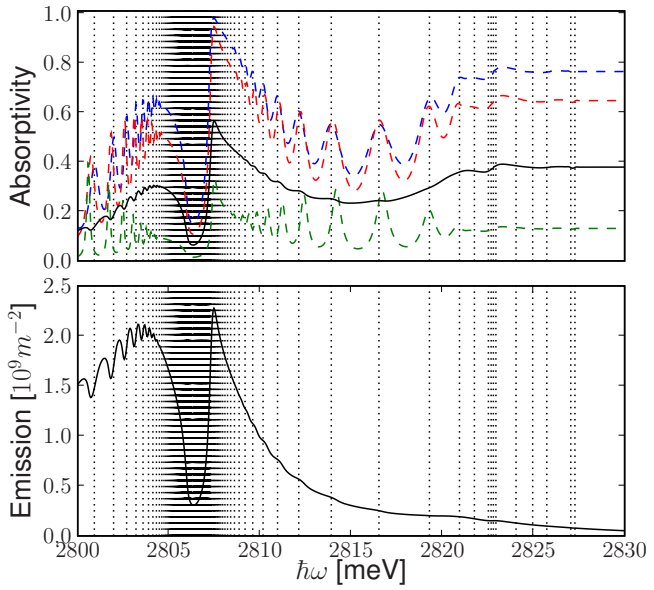

FIG. 4. (Color online) Absorptivity and quasiequilibrium emission in a weakly excited ZnSe slab; $L=2.5$ μm and $\chi^{(2)}(\mathbf{q}=0,\omega)$. Vertical dotted lines mark FPRs for normal incidence. Top: angle-integrated absorptivity $\bar{a}(\omega)$ (solid line; in a.u.) and absorptivity $a(\omega,\mathbf{q}_\parallel)$ (dashed lines) for incidence angles 0°, 45°, and 85°. Bottom: emission $\bar{s}_e(\omega)$.

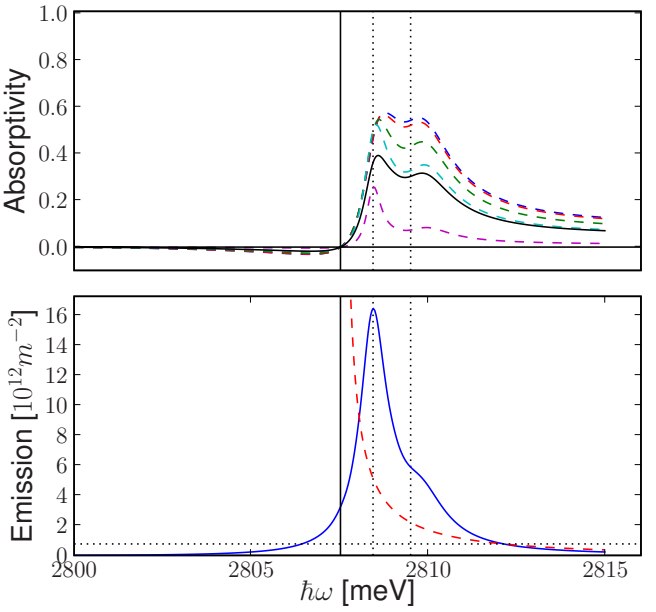

FIG. 5. (Color online) Absorptivity and quasiequilibrium emission in a strongly excited ZnSe slab; $L=50$ nm and $\chi^{(4)}(\mathbf{q}=0,\omega)$. Vertical dotted lines mark FPRs at normal incidence. Solid vertical line marks crossover. Top: angle-integrated absorptivity $\bar{a}(\omega)$ (solid line; in a.u.) and absorptivity $a(\omega,\mathbf{q}_\parallel)$ (dashed lines) for incidence angles 0°, 20°, 45°, 60°, and 85°. Bottom: emission $\bar{s}_e(\omega)$ (solid line) and $b(\omega)$ (dashed line). Scaled dotted horizontal line shows $b=1$ level.

In the spectral region investigated here, it is dominated by the trailer of the Bose function. Even though there is no amplification through gain in this example, there is a considerable emission due to the length of the slab and the nonzero excitation. In view of $b \ll 1$, it is to be considered emission by spontaneous recombination only. For the strongly excited case $\chi^{(4)}$, chemical potential as well as gain are now in the interesting spectral range, and we may expect remarkable amplification and effects arising from the behavior of the Bose function.

At first, we regard the absorption and emission in a short slab ($\chi^{(4)}$, $L=50$ nm, and Fig. 5). In this configuration, Fabry-Perot resonances are sparse and none happens to appear in the gain range. Somewhat uncommonly, the emission is concentrated in the absorbing range at two Fabry-Perot resonances close above the crossover. There is no amplification through gain yet. However, the emission is still higher than in the previous case due to b being greater than unity close to its singularity at the crossover. The emission is thus caused by stimulated recombination and the amplification here an effect of the degeneracy.

This is different in a longer slab, where FPRs exist in the gain range, causing strong peaks in the absorptivity as in Fig. 3(c). Then, the emission is dominated by these peaks (Fig. 6). Weaker structures get lost in the angle integration. The Bose distribution shifts the weight between the peaks and, for modes close to the crossover, amplifies even further. Here, finally, the result is a sharp and strong emission line, while three other modes fall short by more than a magnitude.

C. Mode density

The *density of modes*

$$\rho(\omega) = \int \frac{d^3\mathbf{q}}{(2\pi)^3}\delta(\omega - cq), \tag{76}$$

often called density of states, is an interesting physical quantity for the analysis of the optical properties of materials

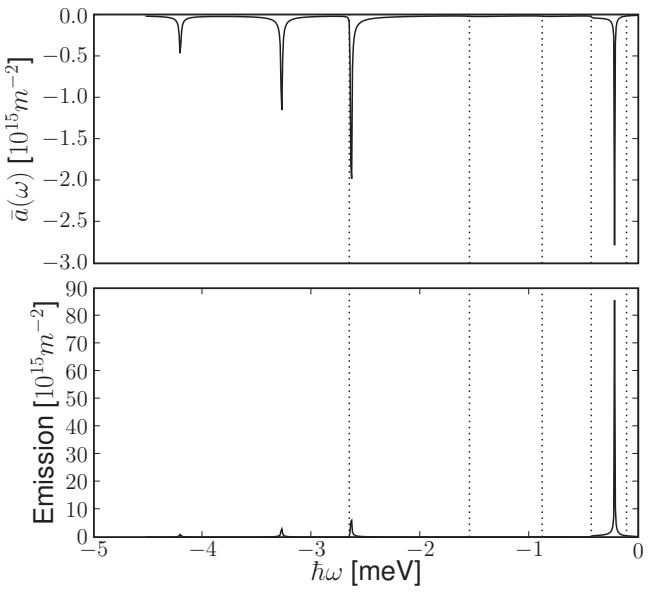

FIG. 6. Angle-integrated absorptivity $\bar{a}(\omega)$ (top) and quasiequilibrium emission $\bar{s}_e(\omega)$ (bottom) for the case of Fig. 3(c). Vertical dotted lines mark FPRs at normal incidence.

because, e.g., it is proportional to the rate of spontaneous emission. Moreover, the density of states plays a key role in studies of photonic band-gap materials, which have drawn considerable attention and promise a wide range of applications.[27–29]

These materials owe their special optical properties to their periodic structure, thus having a strongly inhomogeneous susceptibility. In such matter, the density of states is position dependent [*local* density of states (LDOS)] and difficult to calculate.

For example, in Ref. 29, light propagation in a dielectric structure with periodicity in one spatial direction is analyzed on the basis of Green's functions in an approach considering scattering in infinitely thin planes to circumvent the inhomogeneity problem. With the help of the present theory, this problem can be treated exactly, and moreover the discussion of the LDOS can be extended to excited media. Hence, it seems worthwhile to briefly show how the LDOS can be introduced in the framework of this theory and to show its general behavior in an example calculation using the ZnSe susceptibility functions employed in the preceding examples.

In vacuum, the density of photon states can be expressed in terms of the vacuum spectral function $\hat{D}^0$ [Eq. (38)] and has a constant value

$$\rho^0(\omega) = \int \frac{d^3\mathbf{q}}{(2\pi)^3} \frac{i\omega}{\pi c^2} \hat{D}^0(\mathbf{q},\omega) = \frac{\omega^2}{2\pi^2 c^3}. \tag{77}$$

In slab geometry, the vacuum spectral function must be taken at coordinates $x=x'$ since the Fourier transform of the x component of $\mathbf{q}$ is a $\delta(x)$,

$$\rho^0(x,\omega) = \int \frac{d^2\mathbf{q}_\parallel}{(2\pi)^2} \frac{i\omega}{\pi c^2} \hat{D}^0(x,x,\omega,\mathbf{q}_\parallel) = \frac{\omega^2}{2\pi^2 c^3}. \tag{78}$$

We define a local density of states $\rho(x,\omega)$ in analogy to the above with the full spectral function $\hat{D}$ [Eq. (32)] which decomposes accordingly into a vacuum- and a medium-induced contribution

$$\rho(x,\omega) = \int \frac{d^2\mathbf{q}_\parallel}{(2\pi)^2} \frac{i\omega}{\pi c^2} \hat{D}(x,x,\omega,\mathbf{q}_\parallel) = \rho_v(x,\omega) + \rho_m(x,\omega). \tag{79}$$

Now, Eqs. (54)–(56) allow to calculate ρ from the inner vector potential $A(x)$.

In Fig. 7, $\rho(x,\omega)$ and its components are plotted in the vicinity of the surface of a strongly excited 2.5 μm slab for three characteristic frequencies. Far away from the slab, the local density of states approaches the vacuum level. Closer to the surface, it is distorted and shows damped oscillations inside the slab.

At the frequency where Im $\chi(\omega)$, the microscopic absorption, reaches its maximum (top of Fig. 7), these oscillations are quickly damped out. The vacuum contribution ρ_0 vanishes inside the slab.

At the crossover (middle), $\rho_m \equiv 0$ and $\rho \equiv \rho_v$ because Im $\chi(\omega)=0$; i.e., there is no medium influence. For the same reason, the oscillations survive.

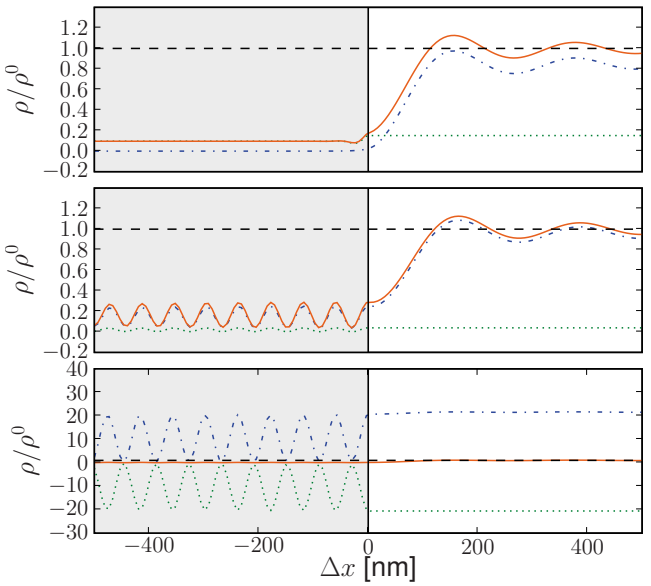

FIG. 7. (Color online) Local density of states $\rho(x,\omega)$ (solid red line), $\rho_v(x,\omega)$ (dash-dotted blue line), and $\rho_m(x,\omega)$ (green dotted line) according to Eq. (79) in the vicinity of the slab surface at $\Delta x=0$ [$\chi^{(4)}(\mathbf{q}=0,\omega), L=2.5$ μm]. Dashed lines mark ρ^0 level at the maximum of Im $\chi(\omega)$ (top), at the crossover, Im $\chi(\omega)=0$ (middle), and in the gain area at a Fabry-Perot resonance (bottom).

On a laser mode (bottom), ρ_v rises two orders of magnitude. ρ_m is negative (because $a<0$) and of the same order such that both nearly compensate to $\rho \approx \rho^0$. Nevertheless, there is a strong emission (see Fig. 6) because the emission is governed by the vacuum-induced contribution $\hat{D}_v$ alone instead of the total spectral function $\hat{D}$.

D. Further application examples

The measurement of the medium excitation distribution b as s_e/a in a ZnSe-ZnSSe heterostructure was demonstrated in Ref. 30. It was found that predominantly polariton modes close to the exciton resonances were occupied in b. Thus, the medium excitation in this case was far from quasiequilibrium. Further experiments are underway to gain more insight into the characteristics of b. Especially, we hope to derive the density and temperature of the excited electron-hole plasma.

Also, with the help of this theory, it was possible to close a gap between rigorous microscopic theory for radiation-matter systems and quantum optics by a clear physical interpretation for the noise current operators appearing in the latter. On this footing, the propagation of nonclassical light through absorbing and dispersing media can be described.[31]

VI. CONCLUSION

Using a quantum-kinetic many-body approach, exact results have been presented for the interacting system of field and matter in a specified geometry. The spectral function of photons splits up into a vacuum-induced and a medium-induced contribution [see Eqs. (32) and (35)], for which the explicit expressions (55) and (56), respectively, have been

obtained. It is noteworthy that both kinds of states are globally (i.e., inside *and* outside) defined and their split does not correspond to a spatial separation of the inside from the outside. There are, of course, many different options to split up the spectral function of photons, e.g., into the one of the pure vacuum $\hat{D}_{\mathrm{vac}}$ and the remaining. But only the decomposition according to Eqs. (32) and (35) yields an exact cancellation of the medium-induced contribution in the balance (58) and so the physically clear and simple structure of the energy flow in Eq. (62).

Also, according to Eq. (61), the field fluctuations split up into a vacuum-induced and a medium-induced contribution whose strengths are given by the distributions n and b, respectively, and only the former contribute to energy transport between the medium and its environment. The distribution n describes the population of the vacuum-induced states and is externally given through preparation of the surrounding, e.g., either as a heat bath or by incoherent radiation incident from outside. Measuring the net energy flow $s_a=-na$ induced by an incoherent radiation n incident from the outside provides the absorption a just as a classical (coherent) transmission-reflection experiment.

The distribution b describes the population of the medium-induced states. It is fixed by the steady-state excitation conditions of the medium and characterizes its globally defined transverse optical excitations as, e.g., excitonic polaritons in semiconductors. For a medium in thermal equilibrium, b tends toward a Bose function, to which a chemical potential can be attributed in the case of quasiequilibrium. Thus, in a sense, real photons, i.e., after their interaction with the fermions of the medium is exactly considered, behave statistically like ideal bosons. For example, for semiconductors, this applies likewise to optical excitations below (excitonic polaritons) and above the fundamental gap, whereas neither excitons nor ionized electron-hole pairs can be regarded as (ideal) bosons. For $n=0$, i.e., pure vacuum in the surrounding, emission is governed by the distribution b. It generalizes the Planck distribution for ideal photons in thermodynamic equilibrium to interacting ones in nonequilibrium.

Our results prove that even lasing can be regarded as quasithermal emission. This has already been demonstrated in Ref. 4 neglecting spatial dispersion and is now exactly confirmed. All the features of this light result exclusively from an extremely strong renormalization of the globally defined coherent absorption a in the gain region due to high compensation of output losses there. Such quasithermal emission has been discussed in sample calculations for semiconductor slabs at different levels of quasiequilibrium excitation. Furthermore, the emission out of a quantum condensate was shown to appear as an additional sharp peak at the crossover point, whereas no significant structures are expected in the absorption.

As a challenge for both experimentalists and theorists, the nonequilibrium distribution b can be observed directly measuring emission and absorption simultaneously[30] or has to be computed, respectively, providing reasonable approximations for the polarization function.

ACKNOWLEDGMENTS

The authors would like to thank current and former members of the semiconductor theory group at the University of Rostock. This work was supported by the Deutsche Forschungsgemeinschaft (Sonderforschungsbereich 652).

APPENDIX A: SYMMETRIES AND IDENTITIES IN THE PHOTON GREEN'S FUNCTION

The most important Green's function identities are given in Eqs. (14) and (21). More identities are listed, e.g., in Refs. 12 and 14.

Additional useful symmetries in the steady-state slab geometry are as follows: (I) as a result of the Fourier transformations,

$$D^{\mathrm{ret}}(x,x',\omega,\mathbf{q}_\parallel)=D^{\mathrm{ret}}(x,x',-\omega,-\mathbf{q}_\parallel)^*=D^{\mathrm{adv}}(x',x,\omega,\mathbf{q}_\parallel)^*, \tag{A1}$$

$$D^{>}(x,x',\omega,\mathbf{q}_\parallel)=D^{<}(x',x,-\omega,-\mathbf{q}_\parallel)=-D^{>}(x',x,\omega,\mathbf{q}_\parallel)^*, \tag{A2}$$

$$\hat{D}(x,x',\omega,\mathbf{q}_\parallel)=\hat{D}(x,x',-\omega,-\mathbf{q}_\parallel)^*=-\hat{D}(x',x,-\omega,-\mathbf{q}_\parallel), \tag{A3}$$

(II) due to symmetry in the geometry,

$$D^{\gtrless}(x,x',\omega,\mathbf{q}_\parallel)=D^{\gtrless}(-x,-x',\omega,\mathbf{q}_\parallel), \tag{A4}$$

(III) and if $\chi(x,x',\omega,\mathbf{q}_\parallel)=\chi(x',x,\omega,\mathbf{q}_\parallel)$,

$$\hat{D}(x,x',\omega,\mathbf{q}_\parallel)=2\mathrm{i}\ \mathrm{Im}\ D^{\mathrm{ret}}(x,x',\omega,\mathbf{q}_\parallel). \tag{A5}$$

In this paper, the medium is assumed to be isotropic for simplicity. Then, the GFs depend only on the norm of $\mathbf{q}_\parallel$ so that it becomes an outer parameter. Due to the Dyson equation, these symmetries and identities also apply for the inverse Green's function and the polarization function.

APPENDIX B: GREEN'S FUNCTION REPRESENTATION OF THE SYMMETRIZED DISSIPATION W

The operator correlations appearing in the symmetrized dissipation $\langle\hat{W}\rangle=\langle(\hat{\mathbf{j}}\cdot\hat{\mathbf{E}})_{\mathrm{sym}}\rangle$ can be conveniently handled on the double-time contour

$$W_{\mathcal{C}}(\underline{1},\underline{2})=-\frac{\partial}{\partial\underline{t}_2}\langle j(\underline{1})A(\underline{2})\rangle, \tag{B1}$$

$$W^{>}(1,2)\big|_{1=2}=\langle j(1)E(1)\rangle, \tag{B2}$$

$$W^{<}(1,2)\big|_{1=2}=\langle E(1)j(1)\rangle. \tag{B3}$$

Since, in analogy to Eq. (8),

$$\langle j(\underline{1})A(\underline{2})\rangle=\frac{\hbar}{\mathrm{i}}\frac{\delta j_{\mathrm{ind}}(\underline{1})}{\delta j_{\mathrm{ext}}(\underline{2})}+j_{\mathrm{ind}}(\underline{1})A_{\mathrm{eff}}(\underline{2}) \tag{B4}$$

follows for $A_{\mathrm{eff}}=0$,

$$\langle j(\underline{1})E(\underline{1})\rangle=\left\{\mathrm{i}\hbar P(\underline{1},\underline{3})\frac{\partial}{\partial\underline{t}_2}D(\underline{3},\underline{2})\right\}_{1=2} \tag{B5}$$

and we can establish the physical limit with the help of the Langreth theorem,[12]

$$W(1) = \frac{1}{2}\left\{ i\hbar \frac{\partial}{\partial t_2}[P^{++}(1,3)D^{>}(3,2) - P^{>}(1,3)D^{--}(3,2) + P^{<}(1,3)D^{++}(3,2) - P^{--}(1,3)D^{<}(3,2)] \right\}_{1=2}. \tag{B6}$$

Using Green's function identities, the contents of the square brackets can be transformed to (some parameters suppressed in the following)

$$[\cdots] = \Theta(t_1 - t_3)(P^{>} - P^{<})(D^{>} + D^{<}) - \Theta(t_2 - t_3)(P^{>} + P^{<})(D^{>} - D^{<}). \tag{B7}$$

Replacing $\Theta(t_2-t_3)=\Theta(t_1-t_3)+[\Theta(t_2-t_3)-\Theta(t_1-t_3)]$, one finds that the second term vanishes under $\partial/\partial t_2 \int dt_3$ due to temporal homogeneity (especially, $D^{>}(t_2-t_2)-D^{<}(t_2-t_2) = \langle A(t_2)A(t_2)\rangle - \langle A(t_2)A(t_2)\rangle = 0$ in the $1 \to 2$ limit). The remainder

$$\frac{\partial}{\partial t_2}[\cdots] = 2\frac{\partial}{\partial t_2}\int d^3\mathbf{r}_3 dt_3 \Theta(t_1 - t_3)[P^{>}(t_1 - t_3)D^{<}(t_3 - t_2) - P^{<}(t_1 - t_3)D^{>}(t_3 - t_2)] \tag{B8}$$

can be Fourier transformed. The step function yields a Dirac identity in Fourier space (Sokhotsky-Weierstrass theorem) such that we have in slab geometry ($\mathbf{q}_\parallel$ integral omitted)

$$\begin{aligned} W(1) &= \frac{1}{2} i\hbar \frac{\partial}{\partial t_2}[\cdots] \\ &= -i\hbar \int dx_3 \mathcal{P} \int \frac{d\omega_1}{2\pi} \int \frac{d\omega_2}{2\pi} \frac{\omega_2}{\omega_2 - \omega_1} \\ &\quad \times [P^{>}(\omega_1)D^{<}(\omega_2) - P^{<}(\omega_1)D^{>}(\omega_2)] \\ &\quad - \frac{1}{2}\int dx_3 \int \frac{d\omega}{2\pi} \hbar\omega \\ &\quad \times [P^{>}(\omega)D^{<}(\omega) - P^{<}(\omega)D^{>}(\omega)]. \end{aligned} \tag{B9}$$

The principal-value term vanishes under the x integral to be taken for Eq. (43). Employing Eq. (37) results in ($\omega, \mathbf{q}_\parallel$ integrals omitted, $(1)=(x_1)$, and all integrals run from $-L/2$ to $L/2$)

$$\begin{aligned} -\int d1 W(1) &= \frac{1}{2}\int d1 \int d2 \int d3 \int d4 [P^{>}(1,2)D^{\mathrm{ret}}(2,3) \\ &\quad \times P^{<}(3,4)D^{\mathrm{adv}}(4,1) + n^{<}P^{>}(1,2)\hat{D}_v(2,1) \\ &\quad - P^{<}(1,2)D^{\mathrm{ret}}(2,3)P^{>}(3,4)D^{\mathrm{adv}}(4,1) \\ &\quad - n^{>}P^{<}(1,2)\hat{D}_v(2,1)]. \end{aligned} \tag{B10}$$

With the help of GF symmetries, one can show that the $PDPD$ terms vanish. The complete result is

$$\begin{aligned} -\int_V dx W(x) &= \int_0^\infty \frac{d\omega}{2\pi}\hbar\omega \int \frac{d^2\mathbf{q}_\parallel}{4\pi^2} \int dx_1 \int dx_2 \\ &\quad \times [n^{<}P^{>}(x_1,x_2)\hat{D}_v(x_2,x_1) \\ &\quad - n^{>}P^{<}(x_1,x_2)\hat{D}_v(x_2,x_1)]. \end{aligned} \tag{B11}$$

*felix.richter2@uni-rostock.de

[1] P. C. Martin and J. Schwinger, Phys. Rev. **115**, 1342 (1959).
[2] L. P. Kadanoff and G. Baym, *Quantum Statistical Mechanics* (Benjamin, New York, 1962).
[3] L. V. Keldysh, Zh. Eksp. Teor. Fiz. **47**, 1515 (1964) [Sov. Phys. JETP **20**, 1018 (1965)].
[4] K. Henneberger and S. W. Koch, Phys. Rev. Lett. **76**, 1820 (1996).
[5] K. Henneberger and S. W. Koch, in *Microscopic Theory of Semiconductors: Quantum Kinetics, Confinement and Lasers*, edited by S. W. Koch (World Scientific, Singapore, 1995), pp. 131–166.
[6] K. Henneberger, Phys. Status Solidi B (to be published).
[7] F. Meinke, Ph.D. thesis, University of Rostock, 2005.
[8] G. Kirchhoff, Ann. Phys. **185**, 275 (1860).
[9] M. Planck, Ann. Phys. **309**, 553 (1901).
[10] L. V. Keldysh, in *Progress in Nonequilibrium Green's Functions II*, edited by M. Bonitz and D. Semkat (World Scientific, Singapore, 2003), pp. 4–17.
[11] K. Henneberger and H. Haug, Phys. Rev. B **38**, 9759 (1988).
[12] H. Haug and A.-P. Jauho, *Quantum Kinetics in Transport and Optics of Semiconductors*, Springer Series in Solid-State Sciences Vol. 123 (Springer, Berlin, 1996).
[13] D. Kremp, M. Schlanges, and W.-D. Kraeft, *Quantum Statistics of Nonideal Plasmas*, Atomic, Optical, and Plasma Physics Vol. 25 (Springer, Berlin, 2005).
[14] D. F. DuBois, in *Lectures in Theoretical Physics*, edited by W. E. Brittin (Gordon and Breach, New York, 1967), Vol. 109, pp. 469–620.
[15] G. D. Mahan, *Many-Particle Physics*, 2nd ed. (Plenum, New York, 1993).
[16] H. Haug and S. W. Koch, *Quantum Theory of the Optical and Electronic Properties of Semiconductors*, 4th ed. (World Scientific, Singapore, 2004).
[17] F. Richter, M. Florian, and K. Henneberger, Europhys. Lett. **81**, 67005 (2008).
[18] P. Halevi, *Spatial Dispersions in Solids and Plasma* (North-Holland, Amsterdam, 1992).
[19] K. Henneberger, arXiv:0810.5058 (unpublished).
[20] A. A. Maradudin and D. L. Mills, Phys. Rev. B **7**, 2787 (1973).
[21] R. Kubo, J. Phys. Soc. Jpn. **12**, 570 (1957).
[22] P. Nozières and S. Schmitt-Rink, J. Low Temp. Phys. **59**, 195 (1985).
[23] F. X. Bronold and H. Fehske, Phys. Rev. B **74**, 165107 (2006).
[24] D. Semkat, D. Kremp, and K. Henneberger, Phys. Status Solidi C (to be published).

[25] D. Kremp, D. Semkat, and K. Henneberger, Phys. Rev. B **78**, 125315 (2008).
[26] M. Seemann, F. Kieseling, H. Stolz, R. Franz, G. Manzke, K. Henneberger, T. Passow, and D. Hommel, Phys. Rev. B **72**, 075204 (2005).
[27] R. Sprik, B. A. van Tiggelen, and A. Lagendijk, Europhys. Lett. **35**, 265 (1996).
[28] Z.-Y. Li and Y. Xia, Phys. Rev. A **63**, 043817 (2001).
[29] M. Wubs and A. Lagendijk, Phys. Rev. E **65**, 046612 (2002).
[30] M. Seemann, F. Kieseling, H. Stolz, M. Florian, G. Manzke, K. Henneberger, and D. Hommel, Phys. Status Solidi B **245**, 1093 (2008).
[31] D. Y. Vasylyev, W. Vogel, K. Henneberger, T. Schmielau, and D.-G. Welsch, Phys. Rev. A **78**, 033837 (2008).